Journal of Sound and Vibration (2001) **241**(3), 337–359
doi:10.1006/jsvi.2000.3302, available online at http://www.idealibrary.com on IDEAL®

STRUCTURAL IDENTIFICATION FROM AMBIENT VIBRATION MEASUREMENT USING THE MULTIVARIATE AR MODEL

C. S. HUANG

Department of Civil Engineering, National Chiao Tung University, Hsinchu, Taiwan, Republic of China. E-mail: cshuang@cc.nctu.edu.tw

(*Received* 8 *December* 1999, *and in final form* 19 *July* 2000)

A procedure for identifying the dynamic characteristics of a structural system using the multivariate AR (ARV) model is presented in the paper. A least-squares approach to determine the coefficient matrices of the ARV model is proposed, which is a modification of the traditional one. The modification is based on the equivalence between the correlation function matrix for the responses of a linear system subjected to white-noise input and the deterministic free vibration responses of the system. Then, the dynamic characteristics of the system are evaluated directly from the coefficient matrices of the ARV model by adopting the concept behind Ibrahim's system identification technique. The superiority of the proposed procedure over the traditional one is demonstrated through numerical studies on a six-story shear building. Finally, the present identification procedure is applied to identify the dynamic characteristics of a three-span highway bridge from its ambient vibration responses subjected to traffic flow. The validity of the present procedure is confirmed by the excellent agreement between the identified results obtained in the present study and those obtained from an impulse test.

1. INTRODUCTION

Investigation of the dynamic characteristics of an existing structure system based on field tests is a necessary and important task in the course of checking the construction quality, validating or improving analytical finite element structural models, or conducting damage assessment. To accomplish this task, the well-known field tests used are ambient vibration tests, forced vibration tests, free vibration tests, and earthquake response measurement. Among these field tests, ambient vibration experiments are the most popular ones because they are portable and easy to set-up. However, because the input in an ambient vibration test is usually too complicated to be known or measured, one has to determine the modal parameters from the output data only. Two main methods have been used in time-domain identification for this purpose. One is a method that incorporates the random decrement technique with the Ibrahim time-domain scheme (ITD) [1, 2] or with the least-squares complex exponential method [3], in which the ambient vibration data are transformed into free decay responses using the random decrement technique. Another method employs the time-series models, AR and ARMA, which regard the ambient vibration responses as random processes of AR or ARMA [4–10]. Among these techniques, the ARMA model is based on the assumption of a stationary input while the others assume that the input is a Gaussian white-noise process. However, estimating the coefficients is more involved for

0022-460X/01/130337 + 23 $35.00/0

the ARMA model than it is for the AR model because the white-noise signal in the ARMA model is also unknown, so a two-stage least-squares approach or non-linear approach has to be used.

Based on the historical development of time series, Yule [11] was the first to propose the AR model of a single variable in 1927. It was not until 1972 that Gersch and his co-workers [4–6] first applied the time-series model to civil engineering. After that, the AR model of a single variable and the multivariate AR (ARV) model were successfully applied in civil engineering projects to identify structural dynamic characteristics by means of ambient vibration experiments [10–13].

Herein, an efficient procedure is proposed to directly determine the dynamic characteristics of a structural system, namely, the natural frequencies, modal damping ratios, and mode shapes, by using the ARV model. The coefficient matrices of the ARV model are evaluated using a least-squares approach, which is a simply modified version of the traditional one. Then, the dynamic characteristics of the structural system are determined from the coefficient matrices of the ARV model by adopting the concept behind Ibrahim's time-domain identification. In the course of developing the procedure, a simple reason based on structural dynamics was discovered which explains why the ARV model can be used to identify the modal parameters of a structural system even though the model is not exactly equivalent to the discrete form for the equations of motion of the structural system.

To validate the proposed system identification procedure, numerical simulations of a six-story shear building subjected to white-noise and low-pass filtered white-noise input were carried out (see Figure 1). In the numerical examples, the obtained results were

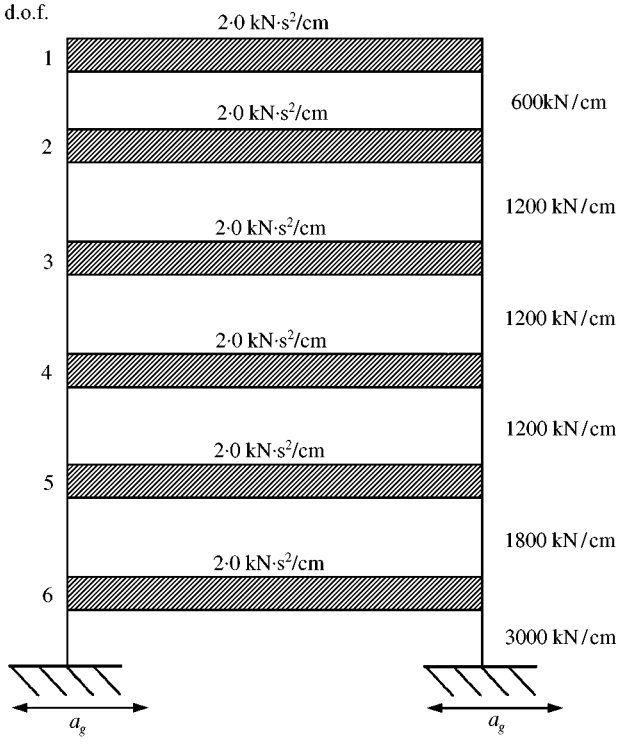

Figure 1. Schematic diagram of a six-story shear building.

compared with those obtained using the traditional least-squares procedure, revealing the superiority of the proposed procedure over the latter.

Finally, the present identification procedure was applied to identify the dynamic characteristics of a three-span highway bridge with pre-stressed concrete box-girders from its ambient vibration measurement subjected to traffic flow. To demonstrate the accuracy of the identified results, the present results were compared with those obtained from an impulse test. Both sets of experimental results were also compared with the finite element solution to show the differences between the experimental and analytical results.

2. ARV MODEL AND STRUCTURAL DYNAMIC RESPONSES

2.1. THE ARV MODEL

The well-known mathematical expression for the ARV model is

$$\{X\}_t = \sum_{i=1}^{n} [\Phi_i]\{X\}_{t-i} + \{A\}_t, \tag{1}$$

where $\{X\}_{t-i}$ is the measured response vector at time $t-i$, $[\Phi_i]$ is a coefficient matrix, and $\{A\}_t$ belongs to a vector white-noise process having the following properties:

$$E[\{A\}_t] = \{0\}, \qquad E[\{A\}_{t-i}\{A\}_{t-j}^{\mathrm{T}}] = \delta_{ij}[W], \tag{2a, b}$$

where $E[\,]$ means the mean-value operation is employed, δ_{ij} is the Kronecker symbol, and $[W]$ is the variance matrix of $\{A\}_t$, which may not be a diagonal matrix. If there are l components in each $\{X\}_t$, then the ARV model represented by equation (1) is denoted as ARV(n; l). Apparently, the ARV model represents a linear relationship between output and white-noise input.

2.2. DISCRETE FORM OF THE DYNAMIC RESPONSE OF A SINGLE-DEGREE-OF-FREEDOM (SDOF) SYSTEM

The equation of motion for a linear s.d.o.f. system is

$$\bar{m}\ddot{q} + \bar{c}\dot{q} + \bar{k}q = f, \tag{3}$$

where $\bar{m}$, $\bar{c}$, and $\bar{k}$ are the mass, damping coefficient, and stiffness of the system, respectively, and f is the input forcing function. The impulse response function for equation (3) with zero initial conditions is

$$h(t) = \frac{1}{\bar{m}\omega_d} \mathrm{e}^{-\zeta\omega t} \sin \omega_d t, \tag{4}$$

where ω is the natural frequency, ζ the damping ratio, and ω_d the damped frequency, which is equal to $\sqrt{(1-\zeta^2)}\omega$.

To build a discrete form equivalent to the continuous-time system of equation (3), we used impulse invariant transformation [14], which preserves the equality of the impulse

function of the continuous-time system with that of the discrete system. Applying Z-transformation to equation (4) yields

$$\tilde{H}(z) = Z[\Delta t\, h(n\Delta t)] = \sum_{n=0}^{\infty} \Delta t\, h(n\Delta t) z^{-n}$$

$$= \frac{\Delta t}{\bar{m}\omega_d} \frac{z^{-1} \mathrm{e}^{-\zeta\omega\Delta t} \sin \omega_d \Delta t}{1 - 2z^{-1} \mathrm{e}^{-\zeta\omega\Delta t} \cos \omega_d \Delta t + z^{-2} \mathrm{e}^{-2(\omega\zeta\Delta t)}}, \tag{5}$$

where $\tilde{H}(z)$ is the Z-transformation of $h(t)$ and Δt is the time increment. Assuming zero initial conditions and applying Z-transformation to the response of equation (3) expressed by the famous Duhamel integral

$$q(t) = \int_{-\infty}^{t} h(t-s) f(s)\, \mathrm{d}s \quad \text{with} \quad f(t) = 0 \quad \text{if } t < 0, \tag{6}$$

yields

$$\tilde{Q}(z) = \tilde{H}(z)\tilde{F}(z), \tag{7}$$

where $\tilde{Q}$ and $\tilde{F}$ are the Z-transformations of q and f, respectively. Substituting equation (5) into equation (7) and performing the inverse of Z-transformation, one obtains [15, 16]

$$q(t) + a_1 q(t-1) + a_2 q(t-2) = \frac{\Delta t}{\bar{m}\omega_d} b_1 f(t-1), \tag{8}$$

where

$$a_1 = -2\mathrm{e}^{-\zeta\omega\Delta t} \cos \omega_d \Delta t, \qquad a_2 = \mathrm{e}^{-2(\zeta\omega\Delta t)}, \qquad b_1 = \mathrm{e}^{-\zeta\omega\Delta t} \sin \omega_d \Delta t. \tag{9a–c}$$

Equation (8) represents the discrete form of the displacement response equivalent to equation (3) based on the requirement of impulse invariance.

Similarly, the equivalent discrete form for the velocity response is

$$\dot{q}(t) + a_1 \dot{q}(t-1) + a_2 \dot{q}(t-2) = \frac{\Delta t}{\bar{m}} f(t) + \frac{\Delta t}{\bar{m}} \bar{b}_1 f(t-1), \tag{10}$$

where

$$\bar{b}_1 = -\left(\frac{\zeta}{\sqrt{1-\zeta^2}} \sin \omega_d \Delta t - \cos \omega_d \Delta t \right) \mathrm{e}^{-\zeta\omega\Delta t}. \tag{11}$$

If the acceleration response is considered, then by differentiating the Duhamel integral (equation (6)) twice with respect to time, replacing t-s with τ, and using causality, one obtains

$$\ddot{q}(t) = \int_0^{\infty} \ddot{h}(\tau) f(t-\tau)\, \mathrm{d}\tau + f(t)\dot{h}(0)$$

$$= \int_0^{\infty} h^*(\tau) f(t-\tau)\, \mathrm{d}\tau, \tag{12}$$

where

$$h^*(t) = \frac{\omega}{\bar{m}} e^{-\zeta\omega t}\left[\frac{2\zeta^2 - 1}{\sqrt{1-\zeta^2}} \sin \omega_d t - 2\zeta \cos \omega_d t\right] + \frac{1}{\bar{m}} \delta(t), \tag{13}$$

$\delta(t)$ is the Dirac delta function, and $h^*(t)$ is the impulse response function for the acceleration response. Again, if one uses impulse invariant transformation, one finds the corresponding discrete form as follows:

$$\ddot{q}(t) + a_1 \ddot{q}(t-1) + a_2 \ddot{q}(t-2) = \hat{b}_1 f(t) + \hat{b}_2 f(t-1) + \hat{b}_3 f(t-2), \tag{14}$$

where

$$\hat{b}_1 = \frac{\Delta t}{\bar{m}}(1 - 2\zeta\omega), \tag{15a}$$

$$\hat{b}_2 = \frac{\Delta t}{\bar{m}}\left\{2(\zeta\omega - 1)\cos \omega_d \Delta t + \frac{(2\zeta^2 - 1)\omega}{\sqrt{1-\zeta^2}} \sin \omega_d \Delta t\right\} e^{-\omega\zeta\Delta t}, \tag{15b}$$

$$\hat{b}_3 = \frac{\Delta t}{\bar{m}} a_2. \tag{15c}$$

It should be noted that equation (14) is different from that derived by Sotoudeh [15], who made a fundamental mistake in his attempt to find the impulse response function for the acceleration response when he left the Dirac delta function out of equation (13).

2.3. DISCRETE FORM OF THE DYNAMIC RESPONSE OF A MULTI-DEGREE-OF-FREEDOM (MDOF) SYSTEM

Let us consider a linear system of N d.o.f.s and assume that the responses of all the d.o.f.s are measured. Using the modal superposition technique and following the procedure described in the preceding section, one can establish the discrete forms for the displacement, velocity, and acceleration responses equivalent to those of the continuous-time system as follows:

$$\{q\}_t = [\hat{\psi}_1]\{q\}_{t-1} + [\hat{\psi}_2]\{q\}_{t-2} + [\hat{\theta}_1]\{f\}_{t-1}, \tag{16a}$$

$$\{\dot{q}\}_t = [\hat{\psi}_1]\{\dot{q}\}_{t-1} + [\hat{\psi}_2]\{\dot{q}\}_{t-2} + [\bar{\theta}_0]\{f\}_t + [\bar{\theta}_1]\{f\}_{t-1}, \tag{16b}$$

$$\{\ddot{q}\}_t = [\hat{\psi}_1]\{\ddot{q}\}_{t-1} + [\hat{\psi}_2]\{\ddot{q}\}_{t-2} + [\tilde{\theta}_0]\{f\}_t + [\tilde{\theta}_1]\{f\}_{t-1} + [\tilde{\theta}_2]\{f\}_{t-2}, \tag{16c}$$

where $[\hat{\psi}_i]$, $\lfloor \hat{\theta}_i \rfloor$, $[\bar{\theta}_i]$, and $[\tilde{\theta}_i]$ are dependent on the mass, damping, and stiffness matrices of the system.

If only the responses of $N_m (N_m < N)$ d.o.f.s of the m.d.o.f. system are measured, then it can be proved that the equivalent discrete form for the measured responses denoted by $\{q_m\}_t$ can be expressed in the following form [16, 17]:

$$\{q_m\}_t = \sum_{i=1}^{p+2} [\hat{\Psi}_i]\{q_m\}_{t-i} + \sum_{j=1}^{p+1} [\hat{\Theta}_i]\{f\}_{t-i}, \tag{17a}$$

$$\{\dot{q}_m\}_t = \sum_{i=1}^{p+2} [\bar{\Psi}_i]\{q_m\}_{t-i} + \sum_{j=0}^{p+1} [\bar{\Theta}_i]\{f\}_{t-i}, \tag{17b}$$

$$\{\ddot{q}_m\}_t = \sum_{i=1}^{p+2} [\tilde{\Psi}_i]\{q_m\}_{t-i} + \sum_{j=0}^{p+2} [\tilde{\Theta}_i]\{f\}_{t-i}, \tag{17c}$$

where $p = 2*(N - N_m)/N_m$ and $(N - N_m)/N_m$ is an integer.

Comparing the discrete forms equivalent to the continuous-time system given in equations (8, 10, 14, 16, 17) with the ARV model reveals that all of the former are different from the latter when the input force terms ($\{f\}_t$) in these equations are replaced with a white-noise vector. As a matter of fact, equations (8, 10, 14, 16, 17) are exactly the same as the multivariate ARMA (ARMAV) model except for the displacement responses when white-noise input is considered. Then, how is it that one can use the ARV model to determine the dynamic characteristics of the continuous-time system? The reason often seen is that the ARV model with infinite order is equivalent to the ARMAV model [18], which means that one can express the responses of a linear system subjected to white-noise input using the ARV model with a sufficiently large order. However, there is another explanation based on the viewpoint of structural dynamics, and it will be given in the next section.

3. EVALUATING COEFFICIENT MATRICES OF ARV MODEL

To evaluate the coefficient matrices of the ARV model, a least-squares approach is usually applied because of its simplicity. Multiplying $\{X\}_{t-k}^{\mathrm{T}}$ by both sides of equation (1) and taking the mean values yields the following relationship for correlation function matrices with different time lags:

$$\mathbf{R}(-k) = \sum_{i=1}^{n} [\Phi_i]\mathbf{R}(i-k), \tag{18}$$

where $\mathbf{R}(k) = E[\{X\}_t\{X\}_{t+k}^{\mathrm{T}}]$. In deriving equation (18), the property of $E[\{A\}_t\{X\}_{t-k}^{\mathrm{T}}] = [0]$ for $k \neq 0$ has been used. Using $\mathbf{R}(-k) = \mathbf{R}^{\mathrm{T}}(k)$, equation (18) becomes

$$\mathbf{R}^{\mathrm{T}}(k) = \sum_{i=1}^{n} [\Phi_i]\mathbf{R}^{\mathrm{T}}(k-i). \tag{19}$$

Conventionally, a procedure often seen in textbooks (i.e., references [19, 20]) is to express equation (19) in the following matrix form:

$$[\hat{R}] = [\tilde{R}][\tilde{\Phi}], \tag{20}$$

where

$$[\hat{R}] = [\mathbf{R}^{\mathrm{T}}(1)\ \ \mathbf{R}^{\mathrm{T}}(2)\ \ \cdots\ \ \mathbf{R}^{\mathrm{T}}(m)]^{\mathrm{T}}, \tag{21a}$$

$$[\tilde{R}] = \begin{bmatrix} \mathbf{R}(0) & \mathbf{R}(-1) & \mathbf{R}(-2) & \cdots & \mathbf{R}(1-n) \\ \mathbf{R}(1) & \mathbf{R}(0) & \mathbf{R}(-1) & \cdots & \mathbf{R}(2-n) \\ \vdots & & & & \\ \mathbf{R}(m-1) & \mathbf{R}(m-2) & \cdots & \cdots & \mathbf{R}(m-n) \end{bmatrix}, \tag{21b}$$

$$[\tilde{\Phi}] = [[\Phi_1]\ \ [\Phi_2]\ \ \cdots\ \ [\Phi_n]]^{\mathrm{T}}. \tag{21c}$$

The value of m is always set much larger than that of n, so a least-squares approach is used to determine the coefficient matrices in equation (21c).

In the present study, a small modification was made to enhance the efficiency of the ARV model in determining the dynamic characteristics of a structural system. The modification is based on the equivalent relationship between the correlation function and free decay responses of the considered structural system. Assume that the input is a white-noise vector with 0 means, and that the coherence functions between the components of the vector are equal to 0 or 1. Huang and Yeh [21] proved that each row of the correlation function matrix $\mathbf{R}(k)$ for the displacement and velocity responses is identical to the free vibration response of the system with certain initial conditions. The equivalent relationship is also valid for acceleration responses if $\mathbf{R}(k)$ is considered with $k > 0$. For example, consider a 2 d.o.f.s linear system with proportional damping described by

$$\begin{bmatrix} M_1 & 0 \\ 0 & M_2 \end{bmatrix} \begin{Bmatrix} \ddot{q}_1(t) \\ \ddot{q}_2(t) \end{Bmatrix} + \begin{bmatrix} C_{11} & C_{12} \\ C_{12} & C_{22} \end{bmatrix} \begin{Bmatrix} \dot{q}_1(t) \\ \dot{q}_2(t) \end{Bmatrix} + \begin{bmatrix} K_{11} & K_{12} \\ K_{12} & K_{22} \end{bmatrix} \begin{Bmatrix} q_1(t) \\ q_2(t) \end{Bmatrix} = - \begin{Bmatrix} M_1 f(t) \\ M_2 f(t) \end{Bmatrix}. \tag{22}$$

Assume that $f(t)$ is white noise with 0 mean and unit auto-spectrum. Based on the definition of the correlation function, one can obtain the following results through lengthy fundamental mathematical operations [2].

When considering displacement responses or velocity responses,

$$\begin{Bmatrix} R_{11}(k) \\ R_{12}(k) \end{Bmatrix} = 2M_1^2 \sum_{i=1}^{2} \mathrm{e}^{-\xi_i \omega_i k \Delta t} (A_i^s \cos(\omega_{di} k \Delta t) + B_i^s \sin(\omega_{di} k \Delta t) \{\phi_i\} \tag{23}$$

and when considering acceleration responses,

$$\begin{Bmatrix} R_{11}(k) \\ R_{12}(k) \end{Bmatrix} = 2M_1^2 \sum_{i=1}^{2} \mathrm{e}^{-\xi_i \omega_i k \Delta t} (A_i^a \cos(\omega_{di} k \Delta t) + B_i^a \sin(\omega_{di} k \Delta t)) \{\phi_i\}$$

$$+ 2M_1^2 \delta(k \Delta t) \sum_{i=1}^{2} C_i^a \{\phi_i\}, \tag{24}$$

where $R_{11}(k)$ and $R_{12}(k)$ are, respectively, the auto-correlation function of the first d.o.f. and the cross-correlation function of the first and second d.o.f.s. ω_i, ω_{di}, ξ_i, and $\{\phi_i\}$ $(i = 1, 2)$ are, respectively, the natural frequencies, damped frequencies, damping ratios, and mode shapes of the system given by equation (22). A_i^s, B_i^s, A_i^a, and B_i^a are constants that depend on the material properties of the system, and their lengthy expressions are given in reference [2]. In equation (24), $\delta(k \Delta t)$ is the Dirac delta function. Obviously, equation (23) is equivalent to a free vibration response of the structural system described by equation (22) with certain initial conditions. When $k > 0$, the second summation terms in equation (24) are equal to 0. Hence, equation (24) with $k > 0$ is also equivalent to a free decay response of the system.

Application of the correlation operation to the ARV model results in equation (19), which happens to be equivalent to the expression of the free decay responses of the continuous-time system if an appropriate value of k is used in equation (19). Consequently, one can use the coefficient matrices of the ARV model to determine the dynamic characteristics of the continuous-time system.

Based on the equivalence relationship between $\mathbf{R}(k)$ and the free decay responses given by Huang and Yeh [21], k has to be larger than or equal to 0. In a real application, the measured responses always contain some noises. If the noises are also similar to white noises, then $\mathbf{R}_m(k) = \mathbf{R}_t(k) + \bar{\delta}(k)[\bar{W}]$, where $\mathbf{R}_m$ and $\mathbf{R}_t$ are the correlation function matrices for measured responses with noises and true responses without noises, respectively, while $[\bar{W}]$ is the variance matrix of the noises, and $\bar{\delta}(k) = 1$ if $k = 0$, $\bar{\delta}(k) = 0$ if $k \neq 0$. Hence, the existence of noise will destroy the equivalence relationship when k is equal to 0. Consequently, it is proposed that equations (21a) and (21b) should be modified to

$$[\hat{R}] = [\mathbf{R}^{\mathrm{T}}(k_i + 1) \quad \mathbf{R}^{\mathrm{T}}(k_i + 2) \quad \cdots \quad \mathbf{R}^{\mathrm{T}}(k_i + m)]^{\mathrm{T}}, \tag{25a}$$

$$[\tilde{R}] = \begin{bmatrix} \mathbf{R}(k_i) & \mathbf{R}(k_i - 1) & \mathbf{R}(k_i - 2) & \cdots & \mathbf{R}(k_i + 1 - n) \\ \mathbf{R}(k_i + 1) & \mathbf{R}(k_i) & \mathbf{R}(k_i - 1) & \cdots & \mathbf{R}(k_i + 2 - n) \\ \vdots & & & & \\ \mathbf{R}(k_i + m - 1) & \mathbf{R}(k_i + m - 2) & \cdots & \cdots & \mathbf{R}(k_i + m - n) \end{bmatrix}, \tag{25b}$$

where $k_i > n - 1$. Based on the author's experience, it is suggested that k_i be selected in the range $k_i \approx n + (4 \sim 14)$ with a sample rate for data measurement of between 50 and 200 Hz. Obviously, when $k_i = 0$, equations (25a) and (25b) are identical to equations (21a) and (21b) respectively.

To determine the coefficient matrices of the ARV model from equations (20), (25a), and (25b), one needs to estimate the correlation function matrix from measured data. The correlation function matrix is often estimated by means of the following equation [20]:

$$\mathbf{R}(k) = \frac{1}{\bar{n}} \sum_{t=1}^{\bar{n}-k} \{X\}_t \{X\}_{t+k}^{\mathrm{T}}, \tag{26}$$

where, usually, $k < \bar{n}/10$.

4. IDENTIFYING THE DYNAMIC CHARACTERISTICS OF STRUCTURES

Comparing the discrete form equivalent to the continuous-time system with the ARV model given in the previous section, one can find that the ARV model without the white-noise term represents a discrete form for free decay responses equivalent to the continuous-time system. Hence, one should be able to determine the dynamic characteristics of the continuous-time system from the coefficient matrices of the ARV model. By adopting the concept behind the Ibrahim time-domain system identification technique, it was proved in references [16, 22] that if one constructs a matrix from the coefficient matrices of the ARV model as follows:

$$[G] = \begin{bmatrix} 0 & I & 0 & 0 & \cdots & 0 \\ 0 & 0 & I & 0 & \cdots & 0 \\ \vdots & & & & & \\ [\Phi_n] & [\Phi_{n-1}] & & & & [\Phi_1] \end{bmatrix}_{2N \times 2N}, \tag{27}$$

where I is a unit matrix by $l * l$, then the dynamic characteristics of the system under consideration can be determined from the eigenvalues and eigenvectors of $[G]$.

In equation (27), $2N = n * l$, where l is the order of $\{X\}_t$. Apparently, each eigenvector of $[G]$ has $2N$ components. Let λ_k be the kth eigenvalue of $[G]$, and let $\{\psi_k\}$ be the corresponding eigenvector. Furthermore, express $\{\psi_k\}^{\mathrm{T}}$ as $\{\psi_k\}_1^{\mathrm{T}} \{\psi_k\}_2^{\mathrm{T}} \ldots \{\psi_k\}_n^{\mathrm{T}})$ with each $\{\psi_k\}_i$ having l components. From

$$[G]\{\psi_k\} = \lambda_k\{\psi_k\}, \tag{28}$$

one can find that

$$\{\psi_k\}_i = \lambda_k\{\psi_k\}_{i-1} \quad (i = 1, 2, \ldots, n), \qquad \sum_{j=0}^{n-1} [\Phi_{n-j}]\{\psi_k\}_{j+1} = \lambda_k\{\psi_k\}_n. \tag{29a, b}$$

The relations given in equation (29a) yield

$$\{\psi_k\} = (\{\psi_k\}_1^{\mathrm{T}}, \lambda_k\{\psi_k\}_1^{\mathrm{T}}, \lambda_k^2\{\psi_k\}_1^{\mathrm{T}}, \ldots, \lambda_k^{n-1}\{\psi_k\}_1^{\mathrm{T}})^{\mathrm{T}}. \tag{30}$$

By substituting equation (29a) into equation (29b), one finds that λ_k has to satisfy the following equation:

$$|\lambda_k^n I - \lambda_k^{n-1}[\Phi_1] - \lambda_k^{n-2}[\Phi_2] \cdots - \lambda_k[\Phi_{n-1}] - [\Phi_n]| = 0. \tag{31}$$

Equation (30) shows that $\{\psi_k\}_i$ and $\{\psi_k\}_j$ for $i, j = 1, 2, \ldots, n$ and $i \neq j$ are parallel to each other. These vectors correspond to a mode shape of the structural system. Equation (31) is usually used to determine the poles of the ARMAV model [7].

The eigenvalue λ_k is usually a complex number, set equal to $a_k + \mathrm{i}b_k$. The frequency and damping ratio of the system are computed by

$$\tilde{\beta}_k = \sqrt{\alpha_k^2 + \beta_k^2}, \qquad \xi_k = -\alpha_k/\tilde{\beta}_k, \tag{32a, b}$$

where

$$\beta_k = \frac{1}{\Delta t} \tan^{-1}\left(\frac{b_k}{a_k}\right), \qquad \alpha_k = \frac{1}{2\Delta t} \ln(a_k^2 + b_k^2), \tag{33a, b}$$

in which Δt is the inverse of the sampling rate of measurement, $\tilde{\beta}_k$ the pseudo-undamped circular natural frequency, and ξ_k is the modal damping ratio.

5. NUMERICAL VERIFICATION

To demonstrate the feasibility of the proposed procedure, Laplace transformation was used to numerically simulate a six-story shear building (see Fig. 1) subjected to white-noise excitation at the base. The simulation was conducted for 5% of the modal damping ratio. The theoretical natural frequencies of the system were 0·801, 2·14, 3·15, 4·25, 5·04, and 5·37 Hz. The velocity and acceleration outputs of the six d.o.f.s with 65 000 data points for each d.o.f were used in the following system identification. The sampling rate of data was 100 Hz.

To check for agreement between the identified mode shapes and theoretical ones, the modal assurance criterion (MAC) proposed by Allemang and Brown [23] was used, which is defined as

$$\mathrm{MAC}(\{\varphi_{iI}, \{\varphi_{iA}\}) = \frac{|\{\varphi_{iI}\}^{\mathrm{T}}\{\varphi_{iA}\}|^2}{\{\varphi_{iI}\}^{\mathrm{T}}\{\varphi_{iI}\}\{\varphi_{iA}\}^{\mathrm{T}}\{\varphi_{iA}\}}, \tag{34}$$

where $\{\varphi_{iI}\}$ is the identified ith mode shape and $\{\varphi_{iA}\}$ is the corresponding analytical mode shape. The value of MAC is between 0 and 1. When the two mode shapes are more similar, the resultant value of MAC is closer to one. On the other hand, when two mode shapes are orthogonal with each other, the resultant MAC value is zero.

It should be noted that in the following numerical examples, when the differences between the identified frequencies and modal damping ratios and the theoretical ones are within 2 and 20%, respectively, and when the MAC values are larger than 0·9, then the identified results will be referred to as "accurate" results. We started with a low order ARV model and then increased the order of the ARV model until we obtained "accurate" results. It should also be noted that other than structural modes, extra spurious modes will occur when the order of the ARV model multiplied by the number of observed d.o.f.s is larger than twice the total number of d.o.f.s of the structural system under consideration. The desired structural modes will consistently occur as the order of the ARV model increases when the order is large enough. The Fourier spectra of the measured responses are also helpful in distinguishing the structural modes from the spurious modes. Sometimes, good engineering judgment has to be practiced to confirm the structural modes.

In the following tables of numerical results, the traditional method means equations (21a) and (21b) were used to evaluate the coefficient matrices of the ARV model while the proposed method means equations (25a) and (25b) were used.

5.1. EFFECTS OF SIGNAL TYPE

In field experiments on ambient vibration, either velocity or acceleration responses are usually measured. By processing the velocity and acceleration responses of all six d.o.f.s from numerical simulation, the "accurate" results shown in Table 1 were obtained using the ARV models with the lowest order.

It can be seen that one has to use a higher order ARV model for acceleration responses than for velocity data to obtain "accurate" estimation of the dynamic characteristics of the system. In comparison with the traditional method, it can be observed that one can use the proposed method with a lower order ARV model to obtain "accurate" results, especially for acceleration data. Consequently, one can save some computer time and effort in distinguishing the true structural modes from the extra spurious modes that are produced due to the use of a high order ARV model.

5.2. EFFECTS OF NOISES

Measured responses always contain some level of corrupted noise. To somewhat simulate this situation, noise with 20% variance of the signal-to-noise ratio was randomly added to the computed responses. The identified results from the noisy velocity responses obtained using different orders of the ARV model are listed in Table 2. The noises in the responses caused difficulty in identifying the higher modes, especially for the modal damping ratio. However, by increasing the order of the ARV model, we could still obtain "accurate" results.

TABLE 1

Identified results obtained using velocity and acceleration responses

Data type	Method	Model	Frequency (Hz)	Modal damping (%)	MAC
Velocity	Traditional	ARV(3; 6)	0·808	4·6	1·00
			2·14	4·8	1·00
			3·15	4·5	1·00
			4·23	4·6	0·98
			5·02	4·3	0·99
			5·41	5·1	0·92
	Proposed	ARV(2; 6)	0·804	4·9	1·00
			2·13	4·8	1·00
			3·14	4·8	1·00
			4·23	5·1	0·98
			5·00	5·2	0·99
			5·36	4·8	1·00
Acceleration	Traditional	ARV(23; 6)	0·802	5·8	1·00
			2·13	4·8	1·00
			3·14	4·8	1·00
			4·23	4·9	0·98
			4·98	5·6	0·96
			5·33	4·7	0·97
	Proposed	ARV(9; 6)	0·806	5·5	1·00
			2·13	5·0	1·00
			3·15	4·9	1·00
			4·23	5·0	0·99
			5·01	5·0	1·00
			5·36	4·9	1·00

Again, to get the same accuracy in the results, the proposed method needs a much lower order ARV model than does the traditional method.

5.3. EFFECTS OF THE NUMBER OF MEASURED DOFS

In practical applications, only the responses for a few d.o.f.s are measured for economic reasons. Table 3 shows the identified results obtained by using the velocity responses of only four and three d.o.f.s of the shear building. The orders of the ARV model listed in the table are the lowest orders resulting in "accurate" results. As expected, a higher order ARV model should be used for fewer measured degrees of freedom. The results given in Table 3 again show that the proposed method can dramatically enhance the efficiency of the ARV model in determining the dynamic characteristics of a structural system.

5.4 EFFECTS OF NON-WHITE-NOISE INPUT

Although the ARV model assumes white-noise input, in practical applications, one often faces situations where the input is similar to bandwidth-limited white-noise. To study the effects of this type of input on ARV modelling, numerical simulation of the six-story shear building was carried out again with a base input of white-noise filtered by a low-pass filter

TABLE 2

Effects of noises on identified results

Model	Method	Frequency (Hz)	Modal damping (%)	MAC
ARV(10; 6)	Traditional	0·854	6·6	1·00
		2·21	6·2	1·00
		3·22	8·2	0·99
		4·57	23·0	0·73
		5·11	12·0	0·11
		†	†	†
	Proposed	0·805	4·7	1·00
		2·13	5·0	1·00
		3·14	5·1	1·00
		4·21	5·5	0·98
		5·04	6·9	0·95
		5·38	9·2	0·94
ARV(20; 6)	Traditional	0·833	5·5	1·00
		2·15	5·0	1·00
		3·08	5·8	0·97
		3·98	14·0	0·58
		4·78	16·0	0·40
		5·58	12·0	0·42
	Proposed	0·805	4·8	1·00
		2·13	4·8	1·00
		3·14	4·9	1·00
		4·23	5·2	0·96
		4·93	6·0	0·98
		5·37	6·6	0·97
ARV(30; 6)	Traditional	0·825	4·8	1·00
		2·11	5·5	0·99
		3·18	9·7	0·97
		4·26	8·0	0·90
		5·21	6·2	0·77
		5·51	15·0	0·17
	Proposed	0·804	4·9	1·00
		2·13	4·6	1·00
		3·13	5·2	1·00
		4·23	4·8	0·96
		4·98	5·8	0·95
		5·43	5·1	0·95

† means no identified data.

shown in Figure 2. In the filter function, the magnitude for $f = f_{cut} + 5$ was about only one-tenth that for $f = f_{cut}$. Figure 3 shows the Fourier spectra of the responses of 1, 2, and 3 d.o.f.s with $f_{cut} = 2$ Hz. Figure 3 reveals that responses for the fifth and sixth modes are two orders of magnitude smaller than the response of the first mode. Table 4 shows the "accurate" results obtained using the lowest order ARV model to process the velocity responses of all the d.o.f.s. As expected, to get identified results with the same accuracy, the order of ARV model needed for the proposed method was significantly lower than that needed for the traditional method. Nevertheless, in spite of using different methods, one can

TABLE 3

Identified results obtained using various measured d.o.f.s

Measured degrees of freedom	(1, 2, 4, 6)		(1, 3, 5)	
Method Model	Traditional ARV(7; 4)	Proposed ARV(4; 4)	Traditional ARV(35; 3)	Proposed ARV(10; 3)
Frequency (Hz)	0·805	0·804	0·804	0·804
	2·13	2·13	2·12	2·13
	3·15	3·14	3·16	3·14
	4·24	4·22	4·26	4·25
	5·05	5·03	4·99	5·01
	5·38	5·37	5·37	5·36
Modal damping (%)	4·8	4·8	4·4	4·9
	5·0	4·5	4·0	4·4
	4·7	4·9	4·8	5·0
	4·8	5·4	5·2	5·4
	4·5	5·3	4·5	5·4
	5·8	5·2	4·0	5·3
MAC	1·00	1·00	1·00	1·00
	1·00	1·00	1·00	1·00
	1·00	1·00	1·00	1·00
	0·99	0·98	0·97	0·98
	1·00	1·00	0·95	1·00
	0·99	1·00	1·00	0·99

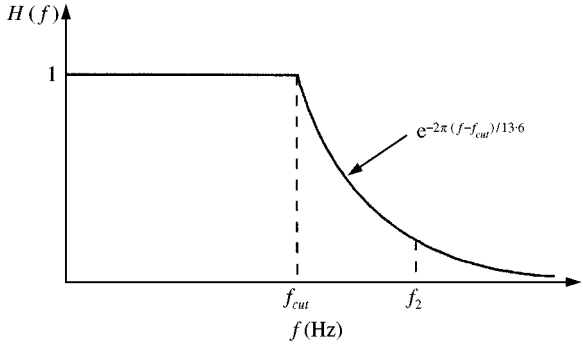

Figure 2. Low-pass filtering function.

apply the ARV model to determine "accurately" the dynamic characteristics of a system by appropriately increasing its order when the input is not white noise.

6. APPLICATION TO AMBIENT VIBRATION MEASUREMENT

To demonstrate the applicability of the proposed procedure to ambient vibration measurement, the measured data for a newly constructed elevated freeway bridge were processed. The bridge, 360 m long, is composed of three-span continuous pre-stressed concrete box-girders with varying cross-sectional area (see Figure 4).

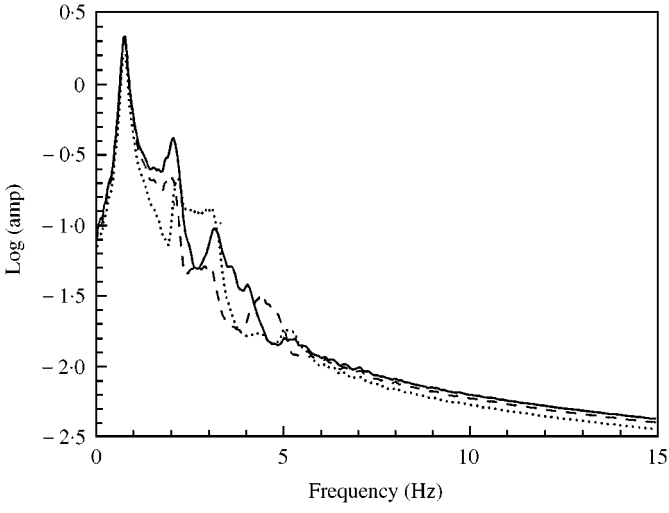

Figure 3. Fourier spectra for the 1st, 2nd and 3rd d.o.f.s with $f_{cut} = 2$ Hz: —— 1st d.o.f.; – – – –2nd d.o.f.; ..... 3rd d.o.f.

TABLE 4

Effects of low-pass filtered white-noise input

f_{cut} (Hz)	2		5	
Method Model	Traditional ARV(6; 6)	Proposed ARV(4; 6)	Traditional ARV(6; 6)	Proposed ARV(2; 6)
Frequency (Hz)	0·804	0·804	0·804	0·805
	2·13	2·12	2·12	2·13
	3·14	3·14	3·14	3·14
	4·25	4·23	4·23	4·23
	5·02	5·02	4·99	4·97
	5·42	5·35	5·32	5·34
Modal damping (%)	5·2	4·8	5·0	4·7
	4·5	4·6	4·9	4·6
	5·1	5·1	4·9	4·9
	4·8	5·4	5·0	5·0
	4·3	5·0	5·0	4·6
	4·6	5·3	4·6	4·0
MAC	1·00	1·00	1·00	1·00
	1·00	1·00	1·00	1·00
	1·00	1·00	1·00	1·00
	0·99	0·98	0·98	0·98
	0·99	1·00	0·97	0·94
	0·95	0·99	0·97	0·98

6.1. INSTRUMENTATION FOR MEASUREMENT

To measure the ambient vibration of the bridge subjected to traffic flow, eight velocity-type sensors with very high sensitivity were attached at the appropriate locations in

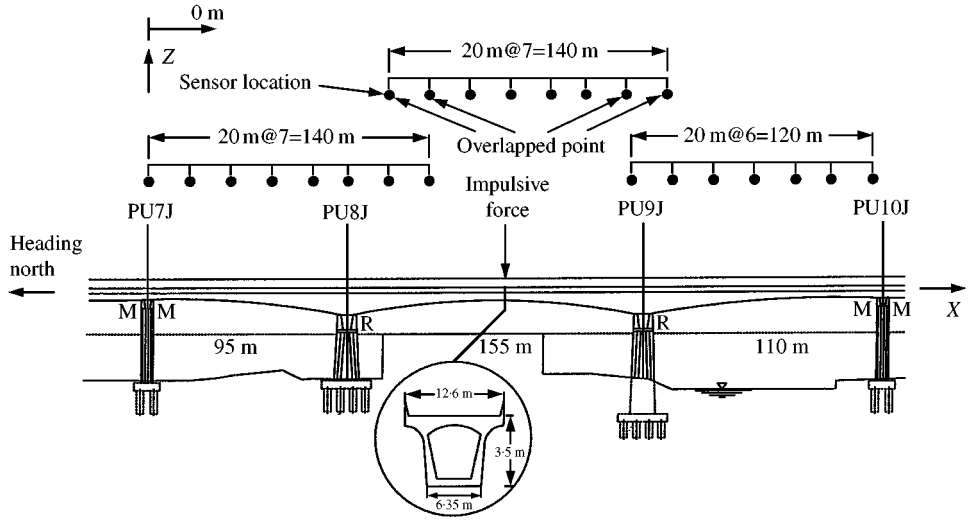

Figure 4. The investigated bridge and the sensor layout.

the box-girder so as not to influence use of the bridge by the public. The analogue sensor signals were converted to digital data and recorded in a PC-based portable data-acquisition system. The resolution for the whole measuring system could reach 10^{-4} cm/s. The data-acquisition system included high- and low-pass filters, whose cut-off frequencies were set equal to 0·1 Hz and one-third of the sampling rate, respectively.

Due to the limited number of sensors available, the responses of the bridge in the longitudinal (x), transverse (y), and vertical (z) directions were independently measured. Furthermore, the measurement in each direction along the bridge was divided into three segments as shown in Figure 4. Eight or seven sensors were deployed at 20 m intervals on each segment. Two measurement stations overlapped for any two adjacent segments so that the mode shapes identified from each segment could be correlated with each other. The ambient vibration responses of the bridge were recorded to 10 min with a sampling rate of 50 Hz.

6.2. RESULTS AND DISCUSSION

The measured velocity responses for each direction and in each segment were processed independently. It should be especially mentioned that the measured responses at the position $x = 0$ (see Figure 4) were found to be smaller than those at the other positions in all directions by 1–2 orders, so the measured data at that position were judged to be abnormal and discarded. The dynamic characteristics of the bridge identified in the present study are listed in Table 5. The results were obtained by using the ARV model with the order between 25 and 40. The listed results occurred consistently as the ARV order increased. Table 5 also shows the results identified in an impulse test using the Ibrahim time-domain system identification technique [24]. The impulse test was carried out about one year before the ambient vibration measurement was done and just before the bridge was opened to the public. The impulse forces were generated at the midpoint of the second span by a loaded truck with a total weight of 14 tons [24]. The measurement arrangement for the impulse test was similar to that for the ambient vibration test. Table 5 also lists the analytical results obtained using the commercial finite element package SAP90 with 89 beam elements for the

TABLE 5
Identified natural frequencies and modal damping ratios

Mode	Ambient test		Impulse test		FEM
	f(Hz)	Damping (%)	f(Hz)	Damping (%)	f(Hz)
1	0·85 (y)	1·4	0·80 (y)	1·3	0·779 (y)
2	0·96 (x, z)	2·6	0·96 (x, z)	3·0	0·854 (y)
3	1·03 (y)	2·3	0·99 (y)	2·7	0·895 (z)
4	1·16 (x)	4·2	1·10 (x)	3·7	0·944 (z)
5	1·24 (y)	3·3	1·23 (y)	5·0	1·10 (y)
6	1·57 (x, y, z)	4·7	1·52 (x, z)	5·1	1·28 (y)
7	1·90 (y)	2·8	1·84 (y)	4·3	1·34 (z)
8	2·21 (z)	4·9	2·15 (z)	6·6	1·66 (y)
9	2·53 (x, y)	3·1	2·51 (x)	4·7	1·70 (z)
10	2·62 (z)	3·2	2·73 (y)	4·6	2·07 (y)
11	2·72 (y)	3·4	3·56 (z)	1·5	2·25 (y)
12	3·62 (y, z)	1·4	3·66 (y)	1·9	2·32 (z)
13	3·76 (y)	3·3	4·00 (y)	3·2	2·50 (x)
14	4·50 (y, z)	2·5	4·36 (z)	1·8	3·12 (y)
15	5·14 (z)	1·9	†	†	3·24 (z)
16	†	†	†	†	3·99 (z)
17	†	†	†	†	4·18 (y)

†means no identified data.

superstructure and 20 beam elements for the piers of the bridge [25]. The input of material and geometrical properties to the analytical finite element model was based on the designed values.

It should be noted that in Table 5, the letters in parentheses in the columns for frequencies indicate the direction(s) of the corresponding vibration mode identified through measurement in that direction. The letter inside the parentheses for the results obtained from finite element analysis denotes the main vibration direction of the corresponding mode. Because the central line of the bridge is neither on the same horizontal plane nor on the same vertical plane, it is expected that the in-plane vibration responses would couple with the out-of-plane ones. Hence, measurement in different directions was expected to result in the same identified frequencies. Indeed, in the analysis of the measured data, we did find that some natural frequencies were repeatedly identified from some sets of measurements in different directions. However, only the direction in which the same natural frequencies could be identified from the measurements in all three segments is indicated in the table for the corresponding vibration mode.

Table 5 shows that 15 modes were identified in the present study in a frequency range from 0 to 5·5 Hz. In the identified frequencies, 13 out of the 15 modes excellently match those obtained through the impulse test with relative differences of less than 5% except for the first mode with 6·3%. The 10th and 15th modes identified through ambient vibration measurement do not have corresponding modes in the impulse test while the 13th mode obtained from the impulse test cannot be identified from the ambient vibration test. Comparing the experimental results with those obtained through finite element analysis, it is found that, generally speaking, the latter do not match the former well and are generally higher than the former.

The agreement between the identified modal damping ratios obtained through the ambient vibration test and the impulse test is not as excellent as that for the identified

frequencies but appears to be reasonably good. The identified modal damping ratios are generally smaller than the designed value of 5%.

The mode shapes that were completely identified through measurement in each direction are shown in Figure 5. The mode shapes corresponding to the same frequency

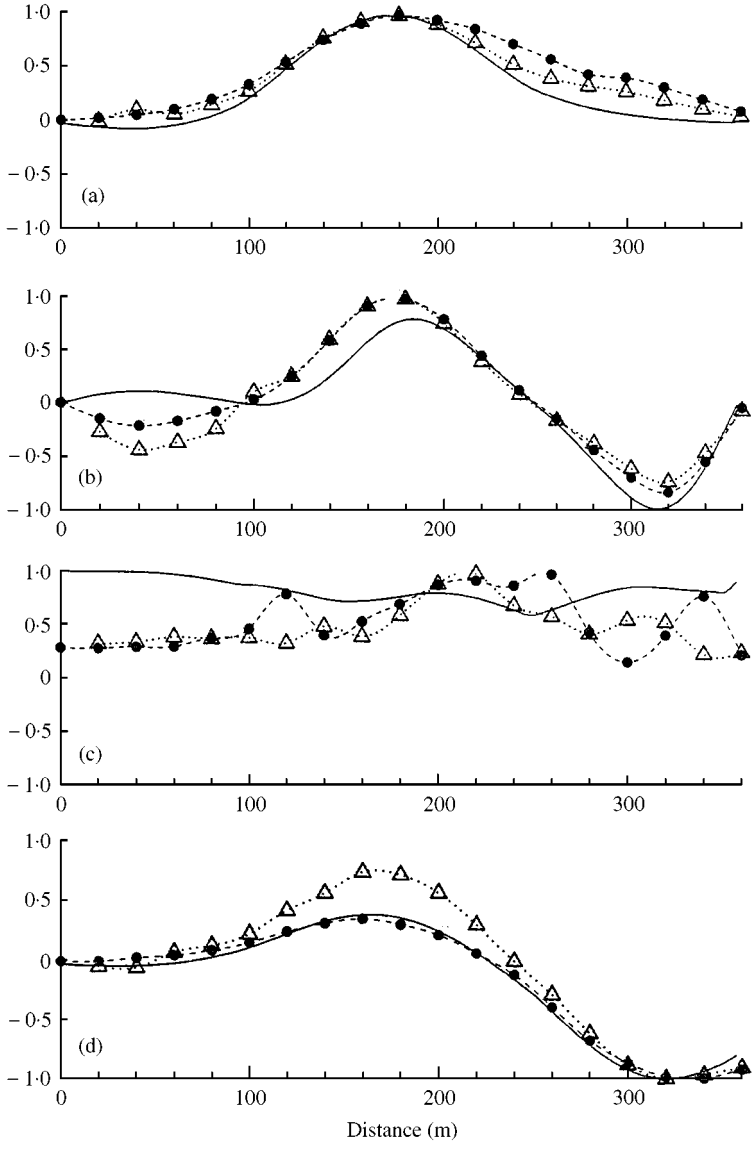

Figure 5. Comparison of identified mode shapes with the finite element results. (a) ———, fem (1y); - - - - ●- - - -, impact (1y); ·····△·····, ambient (1y); (b) ———, fem (3z); - - - - ●- - - -, impact (2z); ·····△·····, ambient (2z); (c) ———, fem (3x); - - - - ●- - - -, impact (2x); ·····△·····, ambient (2x); (d) ———, fem (2y); - - - - ●- - - -, impact (3y); ·····△·····, ambient (3y); (e) ———, fem (4x); - - - - ●- - - -, impact (4x); ·····△·····, ambient (4x); (f) ———, fem (6y); - - - - ●- - - -, impact (5y); ·····△·····, ambient (5y); (g) ———, fem (7z); - - - - ●- - - -, impact (6z); ·····△·····, ambient (6z); (h) ———, fem (7x); - - - - ●- - - -, impact (6x); ·····△·····, ambient (6x); (i) ———, fem (7y); ·····△·····, ambient (6y); (j) ———, fem (8y); - - - - ●- - - -, impact (7y); ·····△·····, ambient (7y); (k) ———, fem (10z); - - - - ●- - - -, impact (8z); ·····△·····, ambient (8z); (l) - - - - ●- - - -, impact (9x); ·····△·····, ambient (9x); ——□——, ambient (9y); (m) ——□——, ambient (10z); - - - - ●- - - -, impact (10y); ·····△·····, ambient (11y); (n) ——□——, ambient (12y); - - - - ●- - - -, impact (11z); ·····△·····, ambient (12z); (o) - - - - ●- - - -, impact (12y); ·····△·····, ambient (13y); ——□——, ambient (14y); (p) - - - - ●- - - -, impact (14z); ·····△·····, ambient (14z); ——□——, ambient (15z).

independently identified through measurements in the three segments were connected to obtain a complete mode shape by using the identified modal data at the overlapping stations for any two adjacent segments. The mode shapes obtained through the impulse test and finite element analysis are also given in Figure 5 if they appear to be similar with those identified through ambient vibration measurement. In the legend for Figure 5, the number inside the parentheses indicates the mode number, and the letter represents the direction of the vibration mode. The values of MAC were computed to quantify the level of consistency between the mode shapes obtained using different methods. Table 6 lists of the values of MAC for the mode shapes identified in the present study versus the corresponding ones obtained through the impulse test and from the finite element program.

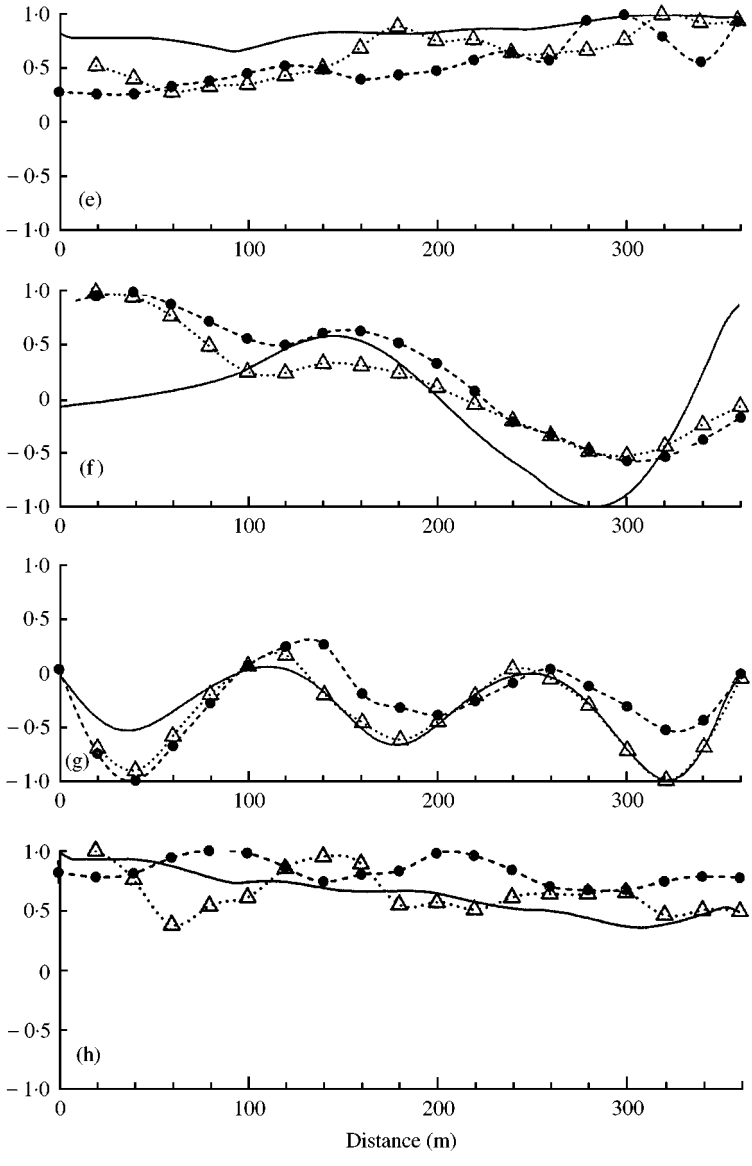

Figure 5. Continued.

Observing the experimental mode shapes shown in Figure 5 and the corresponding MAC values listed in Table 6, one finds that 11 out of the 13 modes that have excellent agreement in frequency show remarkable consistency, especially for lower modes. Comparing the identified mode shapes with those obtained through finite element analysis, one observes that although some of the analytical lower modes match the measured ones very well, it is very hard to find higher modes similar to the measured ones.

The excellent consistency in the identified dynamic characteristics, especially for the lower modes, from the ambient vibration test and the impulse test indicates the validity of the present identification procedure in processing the measured ambient vibration responses in the field. The small discrepancy in the higher modes obtained through the two tests may be due to the fact that the impulse loading in the impulse test was generated at one

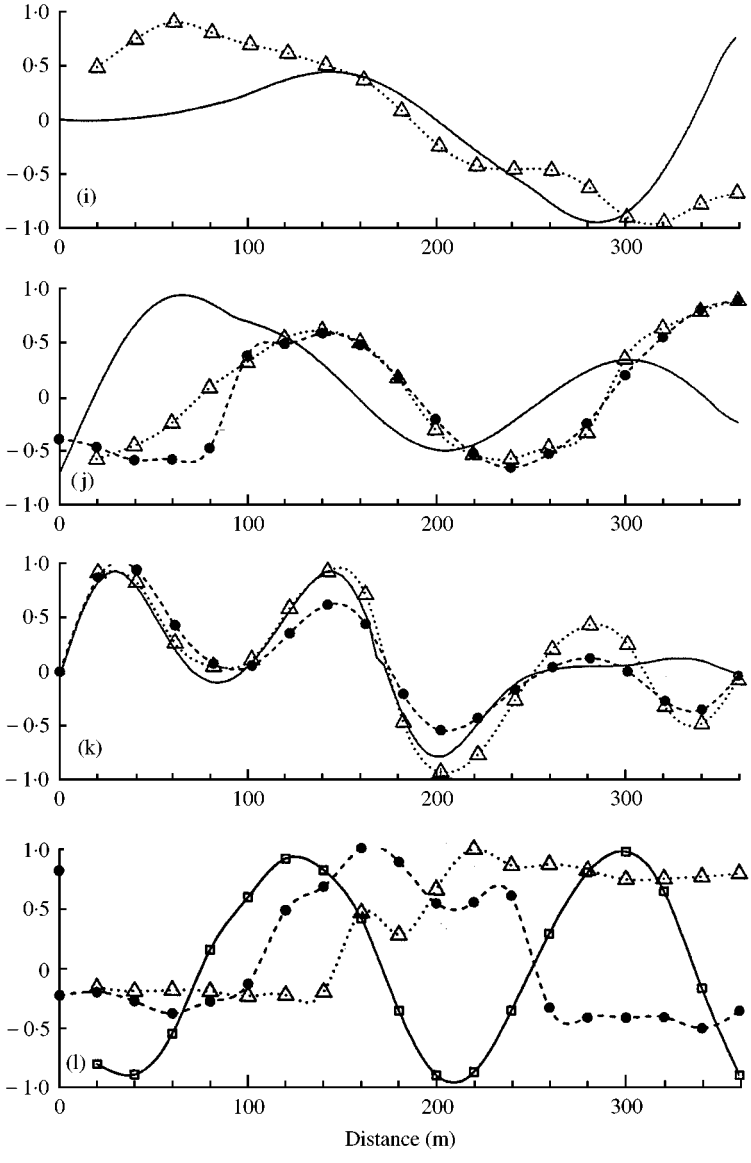

Figure 5. Continued.

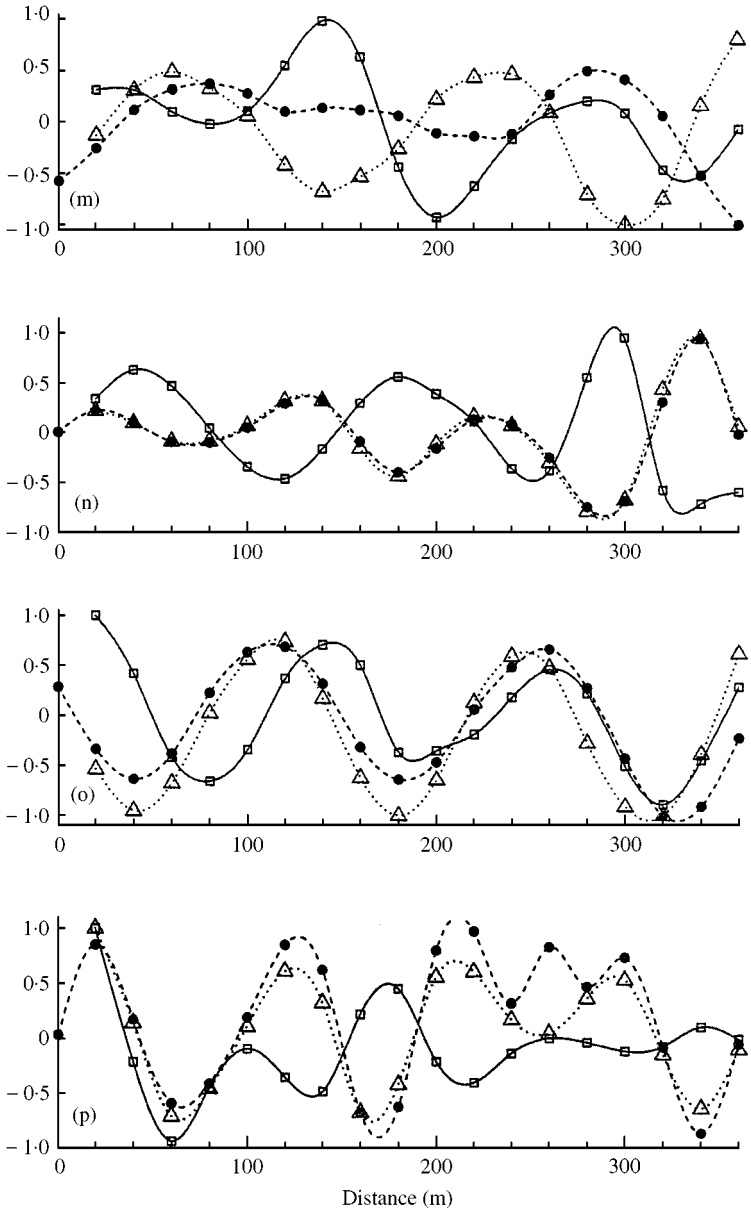

Figure 5. Continued.

point, and also due to the fact that the energy input into the bridge was much smaller than that from traffic flow in the ambient vibration test. As a result, the higher modes were more difficult to identify from the impulse test. This discrepancy in the experimental results could be further investigated by means of forced vibration test. The lack of consistency between the analytical and experiment results indicates that the finite element model should be further refined. As a matter of fact, the identified results obtained in the experiments can serve as a basis for correcting the finite element model using various techniques, such as model updating techniques [26].

TABLE 6
MAC values for the modal shapes obtained using different methods

Ambient vibration test versus impact test			Ambient vibration test versus finite element analysis		
Direction	Mode no. ambient/impact	MAC	Direction	Mode no. ambient/FEM	MAC
Y	1/1	0·981	*Y*	1/1	0·956
Z	2/2	0·965	*Z*	2/3	0·751
X	2/2	0·864	*X*	2/3	0·802
Y	3/3	0·897	*Y*	3/2	0·906
X	4/4	0·924	*X*	4/4	0·943
Y	5/5	0·926	*Y*	5/6	0·235
Z	6/6	0·808	*Z*	6/7	0·941
X	6/6	0·901	*X*	6/7	0·919
Y	7/7	0·901	*Y*	6/7	0·255
Z	8/8	0·890	*Y*	7/8	0·038
X	9/9	0·002	*Z*	8/10	0·836
Y	11/10	0·288	†	†	†
Z	12/11	0·988	†	†	†
Y	13/12	0·767	†	†	†
Z	14/14	0·859	†	†	†

† means that no suitable modal shape, similar to that from the ambient vibration test, was found through finite element analysis.

7. CONCLUDING REMARKS

Although the ARV model does not exactly match the discrete form equivalent to the equations of motion for a structural system from the impulse invariant transform, this paper has provided a simple reason which explains why the ARV model can be successfully applied to identify the dynamic characteristics of a structural system. The reason is mainly based on the equivalence between the correlation function matrix of the responses for a linear system subjected to white-noise input and the free vibration responses of the system. Based on this equivalence relationship, a procedure, which is a modified version of the traditional least-squares approach, has been proposed to efficiently establish the ARV model and dramatically enhance its efficiency in identifying the dynamic characteristics of structures. The dynamic characteristics of a structural system are determined directly from the coefficient matrices of the ARV model by adopting the concept behind the Ibrahim time-domain system identification technique.

To verify the validity of the present identification procedure, numerical simulations of a six-story shear building have been carried out. It has been numerically shown that compared with the traditional least-squares approach, the proposed procedure can dramatically enhance the efficiency in identifying the dynamic characteristics by using a lower order ARV model. In the numerical studies, the effects of several factors were considered so as to simulate a real situation in practical applications. These factors included the signal-type (velocity or acceleration responses), noises, the number of measured d.o.f.s, and non-white-noise input. When acceleration responses, noisy responses, or responses due to non-white-noise input are used, or when the number of measured d.o.f.s is less than the number of d.o.f.s of the system, one has to increase the order of the ARV model to get accurate identification results. The increment in the order of the ARV model is significantly

less when the proposed procedure is used than it is when the traditional least-squares approach is used.

To demonstrate the applicability of the present identification procedure to ambient vibration measurement in the field, the ambient vibration responses of a three-span highway bridge subjected to traffic flow were processed. Fifteen modes were identified in frequencies under 5·5 Hz. Comparing these results with those obtained in an impulse test, excellent agreement has been observed, which indicates the feasibility of using the present procedure in practical applications.

ACKNOWLEDGMENTS

This research was supported by the National Science Council, R. O. C. (NSC88-2711-3-319-200-06). Thanks are extended to former colleagues at the National Center for Research on Earthquake Engineering for valuable discussions.

REFERENCES

1. S. R. Ibrahim and R. S. Pappa 1982 *The AIAA Journal of Spacecraft and Rockets* **19**, 459–465. Large modal survey testing using the Ibrahim time domain identify technique.
2. C. S. Huang, I. C. Tsai and C. H. Yeh 1998 *Journal of the Chinese Institute of Civil and Hydraulic Engineering* **10**, 537–547. Application of random decrement technique to identify the characteristics of a building in time domain from ambient vibration measurement (in Chinese).
3. H. Vold and R. Russell 1983 *Sound and Vibration* **17**, 36–40. Advanced analysis methods improve modal test results.
4. W. Gersch and S. Luo 1972 *The Journal of the Acoustical Society of America* **51**, 402–408. Discrete time series synthesis of randomly excited structural system response.
5. W. Gersch 1974 *Journal of Sound and Vibration* **34**, 63–70. On the achievable accuracy of structural system parameter estimates.
6. W. Gersch and S. Liu 1976 *Journal of Applied Mechanics* **43**, 159–165. Time series methods for synthesis of random vibration systems.
7. Z. N. Wang and T. Fang 1986 *Journal of Applied Mechanics* **53**, 28–32. A time-domain method for identifying modal parameters.
8. L. P. Yong and N. C. Mickleborough 1989 *Journal of Engineering Mechanics, American Society of Civil Engineers* **115**, 2232–2250. Modal identification of vibrating structures using ARMA model.
9. M. Shinozuka, C. B. Yun and H Imai 1982 *Journal of the Engineering Mechanics Division, American Society of Civil Engineers* **108**, 1371–1390. Identification of linear structural dynamic systems.
10. U. Kadakal and O. Yuzugullu 1996 *Soil Dynamics and Earthquake Engineering* **15**, 45–49. A comparative study on the identification methods for the auto-regressive modeling from the ambient vibration records.
11. G. U. Yule 1927 *Philosophical Transactions of the Royal Society of London, Series* A **226**, 267–298. On a method of investigating periodicities in disturbed series, with special reference to Wolfer's sunspot numbers.
12. C. H. Loh and T. S. Wu 1996 *Soil Dynamics and Earthquake Engineering* **15**, 465–483. Identification of Fei-Tsui arch dam from both ambient and seismic response data.
13. X. He and G. De Roeck 1997 *Computer and Structures* **64**, 341–351. System identification of mechanical structures by a high-order multivariate auto-regressive model.
14. L. R. Rabiner and B. Gold 1975 *Theory and Application of Digital Signal Processing*. Englewood Cliffs, NJ: Prentice-Hall.
15. V. Sotoudeh 1986 *Ph.D. Dissertation, Stanford. Stanford University*. Measurement and Analysis of structural vibrations.
16. C. S. Huang 1999 *Report No. NCREE*-99-018, *National Center for Research on Earthquake Engineering, Taipei, Taiwan*. A study on techniques for analyzing ambient vibration measurement (II)—time series methods (in Chinese).

17. J. M. LEURIDAN 1984 *Ph. D. Dissertation. University of Cincinnati, Cincinnati.* Some direct parameter model identification methods applicable for multiple input modal analysis.
18. Z. N. WANG 1984 *Doctoral Thesis, Northwestern Polytechnical University, Shaanxi, China.* Modal analysis of random vibrations and time domain identification of modal parameters.
19. S. M. PANDIT and S. M. WU 1993 *Time Series and System Analysis with Application.* New York: John Wiley & Sons, Inc.
20. S. T. YANG and Y. WU 1989 *Time Series Analysis in Engineering Application.* Hua-Chung Technology University (in Chinese).
21. C. S. HUANG and C. H. YEH 1999 *Mechanical Systems and Signal Processing* **13**, 491–506. Some properties of randomdec signatures.
22. Q. J. YANG, P. Q. ZHANG, C. Q. LIAND and X. P. WU 1994 *Mechanical Systems and Signal Processing* **8**, 159–174. System theory approach to multi-input multi-output modal parameters identification method.
23. R. L. ALLEMANG and D. L. BROWN 1983 *Proceedings of the* 1*st International Modal Analysis Conference, Bethel, Connecticut, U.S.A.*, 110–116. A correlation coefficient for modal vector analysis.
24. C. S. HUANG, Y. B. YANG, L. Y. LU and C. H. CHEN 1999 *Earthquake Engineering and Structural Dynamics* **28**, 857–878. Dynamic testing and system identification of a multi-span highway bridge.
25. I. C. TSAI and J. C. YANG 1996 *Dynamic and Static Monitoring and Analysis of Yuan-Shan Bridge, Second Report to National Freeway Bureau, Ministry of Transportation and Communication, Taiwan.* Dynamic analysis of a freeway bridge subjected to earthquake (in Chinese).
26. J. E. MOTTERSHEAD and M. I. FRISWELL 1993 *Journal of Sound and Vibration* **167**, 347–375. Model updating in structural dynamics: a survey.